STRUCTURAL INTEGRITY ASSESSMENT OF A PROTOTYPE VEHICLE UPPER ARM FOR THE SHELL ECO-MARATHON USING FINITE ELEMENT ANALYSIS

L. H. Hadzri[1], M. R. Mansor[1,*] and Asmawi[2]

[1]Faculty of Mechanical Technology and Engineering,
Universiti Teknikal Malaysia Melaka, Hang Tuah Jaya, 76100 Durian Tunggal, Melaka, Malaysia.

[2]Department of Mechanical Engineering, Faculty of Engineering and Science, Universitas Nasional, Jakarta 12520, Indonesia.

Corresponding Author's Email: [8]muhd.ridzuan@utem.edu.my

Article History: Received 02 September 2025; Revised 26 November 2025; Accepted 29 December 2025

ABSTRACT: The Shell Eco-marathon (SEM) event is a renowned international competition that focuses on bringing university students around the world to design and build vehicles that can achieve the highest possible energy efficiency. Considering that, Universiti Teknikal Malaysia Melaka (UTeM) has allocated its resources to help its automotive engineering students in building highly efficient prototype electric and urban internal combustion engine category vehicles. To achieve so, one key aspect must be considered, which is the weight of the vehicle. In this report, structural analysis was performed on the upper arm using Ansys Student Finite Element Analysis (FEA) under a static bending load condition. The objective is to determine its suitability for the SEM event in terms of strength before committing to topology optimisation. FEA results showed that the upper arm yielded a maximum Safety Factor of 15, and a minimum Safety Factor (SF) of 1.11 and 1.17 for braking and cornering loads, respectively. This signifies that the current material and design is marginally sufficient in terms of safety allowance under both static and SEM dynamic load conditions.

KEYWORDS: *Shell Eco-Marathon (SEM); Highly Efficient; Finite Element Analysis (FEA); Topology Optimization; Safety Factor (SF).*

1.0 INTRODUCTION

The Shell Eco-marathon (SEM) event is a renowned international competition that focuses on challenging university students around the world to design and build vehicles that can achieve the highest possible energy efficiency. Participants will then be able to take their vehicles out on track in the competition to see which team can achieve the highest distance over a set amount of fuel.

Regarding the above, Universiti Teknikal Malaysia Melaka (UTeM) has allocated its resources to help its automotive engineering students in building highly fuel-efficient prototype electric and urban internal combustion engine category vehicles. To achieve this, one key aspect must be considered, which is the weight of the vehicle. As the vehicles are made up of multiple components, key areas for weight improvement are abundant. Research shows that lowering car weight by 10% could result in a fuel economy increase

of about 6-8% which highlights the importance of composite material to achieve the weight reduction and sustainability goal [2].

In essence, lighter vehicles require much less force to move, thereby improving fuel efficiency. Therefore, the upper control arm of the SEM vehicle suspension system was chosen as the prime candidate for topology optimisation to reduce its unsprung mass. Theoretically, a minor weight reduction on the upper arm alone would provide little to no noticeable effect on the ride and handling characteristics of the vehicle. However, when this method is applied to other parts of the vehicle, such as the brake cylinder bracket and wheel knuckle, they collectively provide advantageous weight reduction and, in turn, lessen the fuel consumption of the vehicle.

2.0 METHODOLOGY

The overall research methodology used for this project is summarized in Figure 1. The overall structural analysis process involved the use of two software programs, namely SolidWorks and Ansys Student.

Initially, measurements of the real-life upper arm, as shown in Figure 2 were recorded before designing the geometry model in SolidWorks. The upper arm weighs 0.51 kg, and its dimensions are 251.61 mm (L) x 170 mm (W) x 71.36 mm (H).

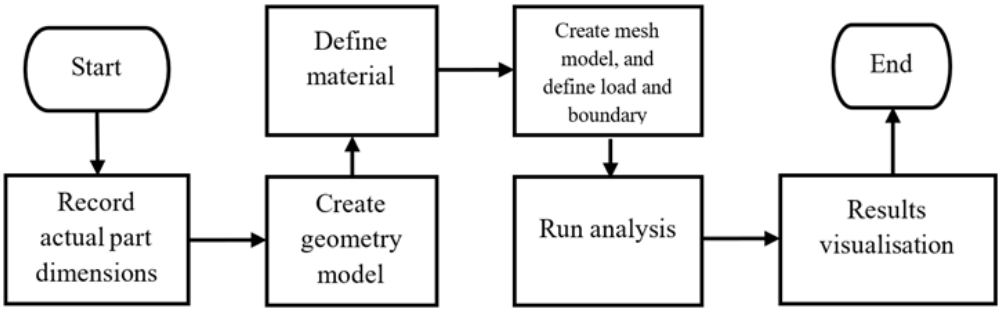

Figure 1: A flow chart of the upper arm structural analysis

Figure 2: The actual design of the upper arm

ISSN 2180-1053 e-ISSN 2289-8123 Vol.17 No.2

Figure 3: The upper arm when installed on the vehicle

An accurate geometry model was then made in SolidWorks as shown in Figure 4, based on its real-life counterpart. The mass of the CAD model is 511.36 grams, as shown in Figure 5, meaning that the design is accurate to the real model.

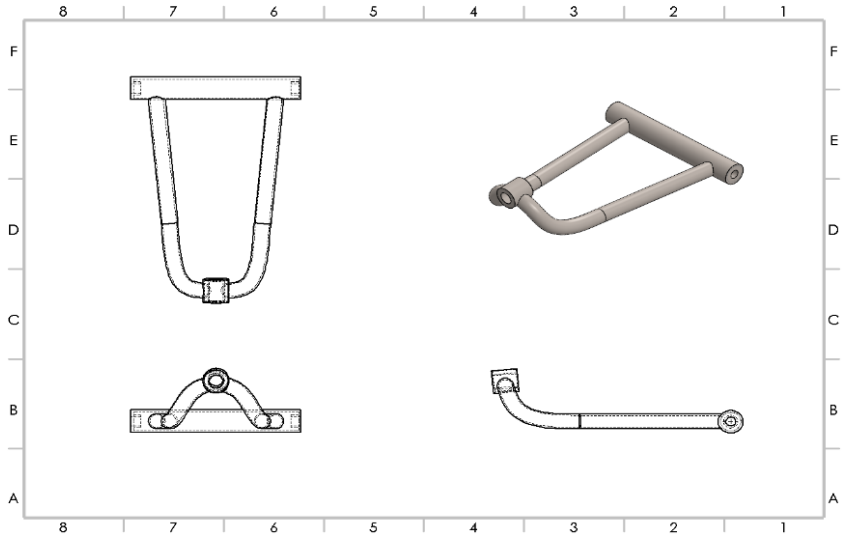

Figure 4: A CAD model of the upper arm, created using SolidWorks

ISSN 2180-1053 e-ISSN 2289-8123 Vol.17 No.2

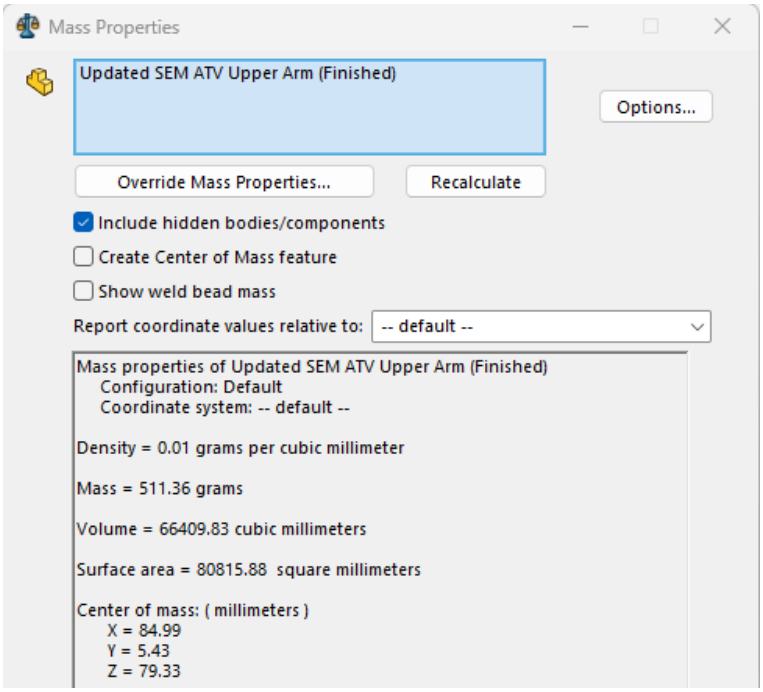

Figure 5: The mass of the upper arm CAD model

ASTM A36 low carbon steel was chosen as the upper arm material due to its low cost, fabrication versatility and high strength – making it the most suitable candidate for a suspension arm material. Figure 6 shows the material properties of ASTM A36 low carbon steel.

Properties of Outline Row 4: ASTM A36

	A	B	C
1	Property	Value	Unit
2	Density	7.85	g cm^-3
3	Isotropic Elasticity		
4	Derive from	Young's Modul...	
5	Young's Modulus	200	GPa
6	Poisson's Ratio	0.26	
7	Bulk Modulus	1.3889E+11	Pa
8	Shear Modulus	7.9365E+10	Pa
9	Tensile Yield Strength	250	MPa
10	Compressive Yield Strength	152	MPa

Figure 6: ASTM A36 material properties defined in Ansys

Next, the geometry model was imported into Ansys Student, and mesh generation was run with the element size of 0.005m as shown in Figure 7.

ISSN 2180-1053 e-ISSN 2289-8123 Vol.17 No.2

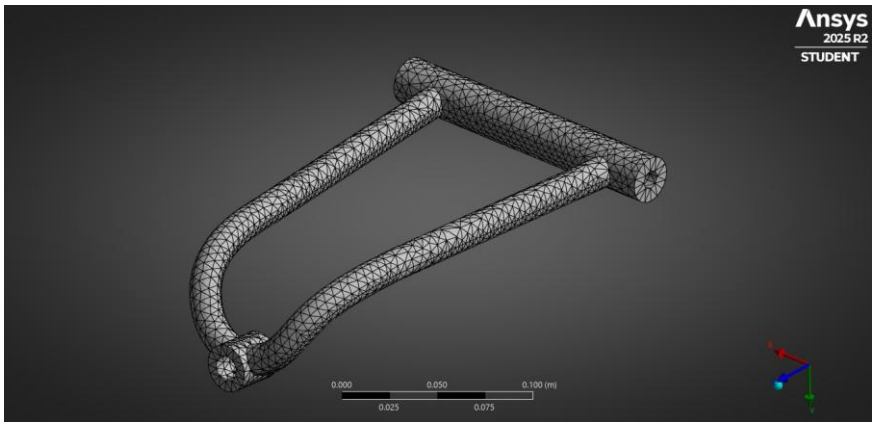

Figure 7: The meshed model of the upper arm

Table 1 shows the vehicle parameters, while Table 2 shows the static load calculation on the front and rear axles, as well as the force acting on one wheel at the front and rear. Due to the rearward position of the driver and the engine, the vehicle is assumed to have a weight distribution of 45:55. The center of gravity height (hcg) is assumed to be 0.5m due to higher ground clearance and height compared to prototype SEM vehicles [3]. Meanwhile, the friction coefficient of 0.85 for dry road was used in this analysis [4]. Next, the Coulomb Friction formula was used to find the maximum friction force and consequently, the deceleration of the vehicle. Finally, based on the 2026 SEM rules and regulations, the vehicle should have a minimum wheelbase of 1.2m and a total weight of 295kg with the driver inside [5].

To find the deceleration of the vehicle, the friction force must first be calculated

$$F_{friction} = \mu W_{total} \quad (1)$$

The deceleration of the vehicle was then obtained using the following formula:

$$a = \frac{F}{m} \quad (2)$$

Table 1: Vehicle parameters

Parameter	Symbol	Value
Assumed weight distribution	-	45:55
Assumed center of gravity height	hcg	0.5 m
Assumed friction coefficient	μ	0.85
Assumed deceleration	a	8.336 m/s^2
Wheelbase	L	1.2 m
Total weight of the vehicle	W = F	225 (vehicle) + 70 (driver) Total = 295 kg = 2892.96 N

The load calculations were obtained using Newton's second law of motion formula:

$$F = ma \quad (3)$$

ISSN 2180-1053 e-ISSN 2289-8123 Vol.17 No.2

Table 2: Load calculations during static conditions

Force acting on the front axle	F_f	132.75 kg = 1302.28 N
Force acting on the rear axle	F_r	162.25 kg = 1591.13 N
Force acting on one wheel of the rear axle	F_{rw}	1591.13/2 = 795.565 N
Force acting on one wheel of the front axle	F_{fw}	1302.28/2 = 651.14 N

A simply supported beam in which F = 2892.96 N acts at a distance X from point F_f was illustrated to find the distance from CG to rear (bcg), as shown in Figure 8. The front wheel braking force (FB), vertical force (FV), and lateral force (FL) was subsequently calculated to simulate the upper arm load conditions during the SEM event. However, static and vertical forces were considered negligible and were not simulated on the upper arm. A study made by Universiti Teknologi Malaysia students shows that the lower arm bears almost all vertical load on the suspension [6]. The dynamic calculations were then performed based on the force calculations made by Shinde, Wangi, and Kaur [7].

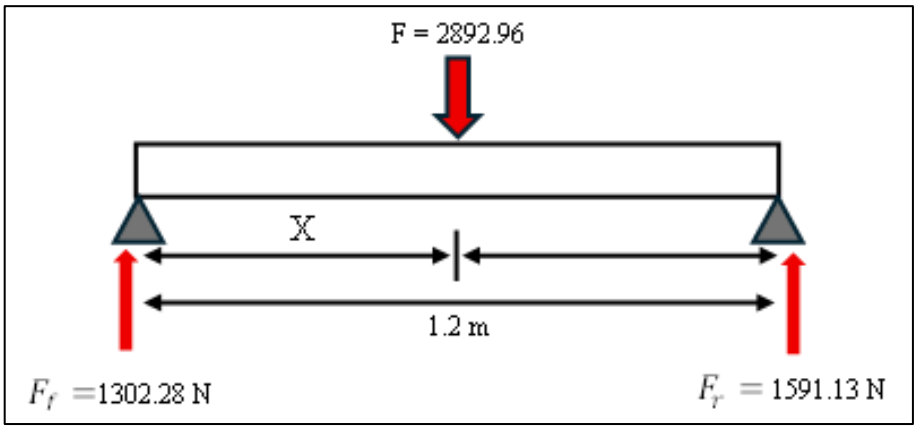

Figure 8: Forces on the front and rear axles, represented by a simply supported beam

To find the front wheel brake force (FB):

$$FB = 0.5\,\mu\,(Static + Dynamic) \tag{4}$$

$$FB = 0.5\,\mu\,\left[\left(W\,.\,\frac{bcg}{L}\right) + \left(m\,.a\,.\frac{hcg}{L}\right)\right] \tag{5}$$

For the front wheel vertical force (FV):

$$FV = \frac{3}{2}\,(Static + Dynamic) \tag{6}$$

$$FV = \frac{3}{2}\left[\left(W\,.\,\frac{bcg}{L}\right) + \left(m\,.a\,.\frac{hcg}{L}\right)\right] \tag{7}$$

The static friction formula was used to calculate the lateral force acting on one wheel:

$$FL = \mu\,.Static \tag{8}$$

ISSN 2180-1053 e-ISSN 2289-8123 Vol.17 No.2

Table 3: Forces calculation

Forces	Values (N)
Front wheel brake force (FB)	988.748
Front wheel vertical force (FV)	3489.698
Front wheel lateral force (FL)	1106.557

For simplicity, the boundary locations of fixed cylindrical support type were specified as in Figure 9, at both ends of the upper arm mounting point. This is done to simulate bolts and nuts fastener type on the actual part.

988.748 N of remote force in the x-axis was then applied on the inner wall of the steering knuckle connector to simulate the braking force acting on the upper arm, as shown in Figure 10.

As shown in Figure 11, 1106.557 N of remote force in the z-axis was applied on the rear side of the wheel knuckle connector to simulate the cornering force being transmitted to the arm by a bolt and nut fastened wheel knuckle.

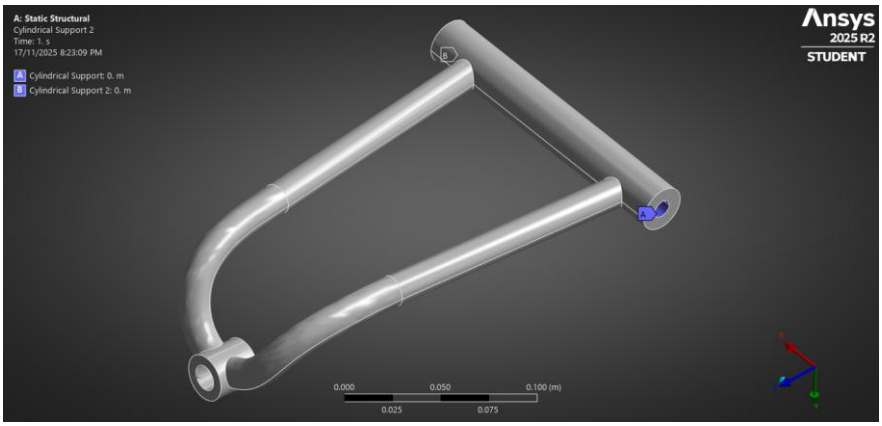

Figure 9: Fixed cylindrical type boundary condition specified at both mounting points

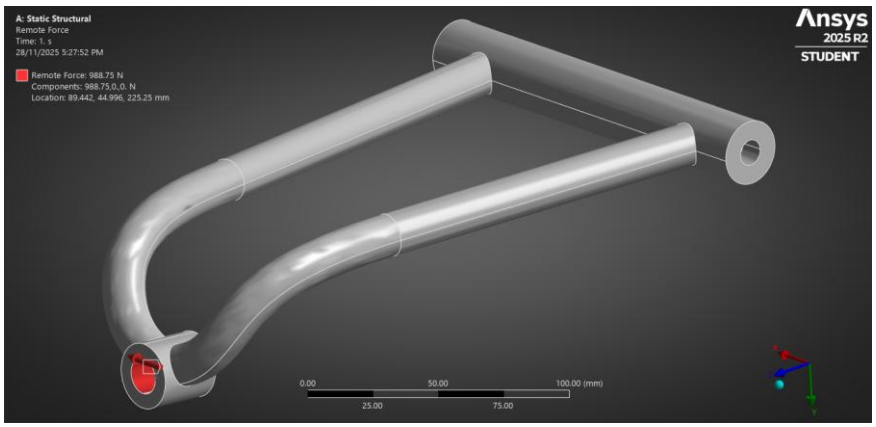

Figure 10: 988.748 N of braking force applied to the connector

ISSN 2180-1053 e-ISSN 2289-8123 Vol.17 No.2

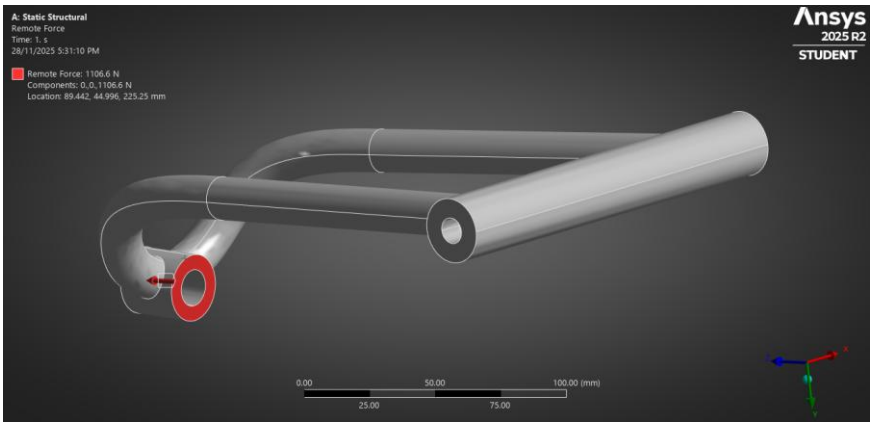

Figure 11: 1106.557 N of lateral force applied to the rear side of the wheel knuckle connector

3.0 RESULTS AND DISCUSSION

The minimum and maximum von Mises stress and total deformation on the upper arm during braking was obtained through the static structural analysis as shown in Figure 12 and Figure 13. The maximum equivalent stress occurs on the left side of the arm near the welding point, reaching a value of 224.36 MPa. On the other hand, the rear side of the pivot arm near the left mounting point only experiences 0.135 MPa minimum stress.

Meanwhile, the maximum total deformation occurs at the bottom side of the wheel knuckle mounting point, yielding up to a value of 1.596 mm from its original position. The pivot arm and the arm area nearby, meanwhile, experienced no deformation whatsoever, as displayed in Figure 13.

Based on the value of von Mises stress, the minimum Factor of Safety value of 1.11 was obtained at the left side of the welding point between the upper arm legs and pivot tube as shown in Figure 14. The maximum FoS value of 15 was obtained at the underside of the wheel knuckle connector. Overall, the FoS value indicates that the upper arm would be able to marginally withstand braking loads under SEM conditions.

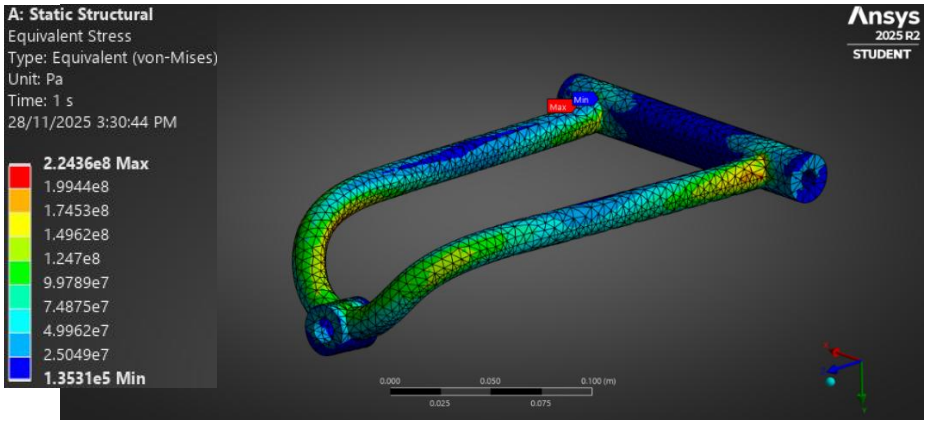

Figure 12: Equivalent stress (von-Mises) distribution under braking force

ISSN 2180-1053 e-ISSN 2289-8123 Vol.17 No.2

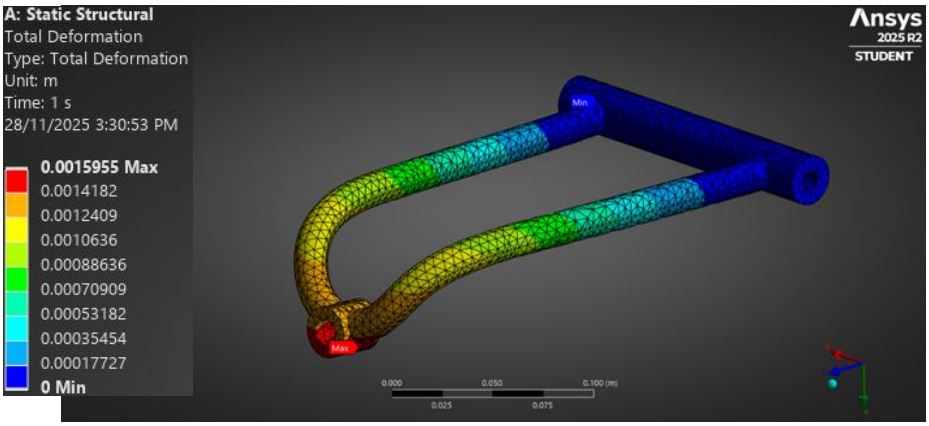

Figure 13: Total deformation distribution under braking force.

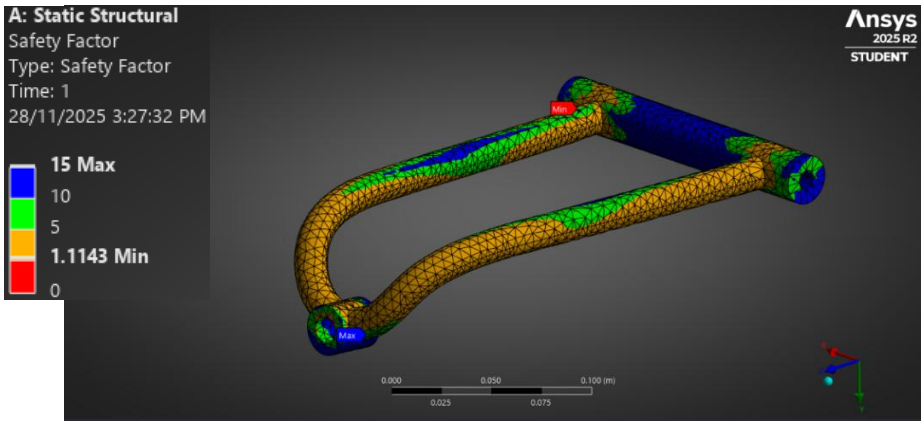

Figure 14: Factor of Safety distribution under braking force.

Following that, the minimum and maximum von Mises stress and total deformation on the upper arm during cornering was also obtained, as shown in Figure 15 and Figure 16. The maximum equivalent stress occurs at the underside of the welding point between the upper arm legs and pivot tube, reaching a value of 212.34 MPa. In contrast, the minimum equivalent stress is found to be at the center of the pivot arm, only reaching a small value of 0.179 MPa.

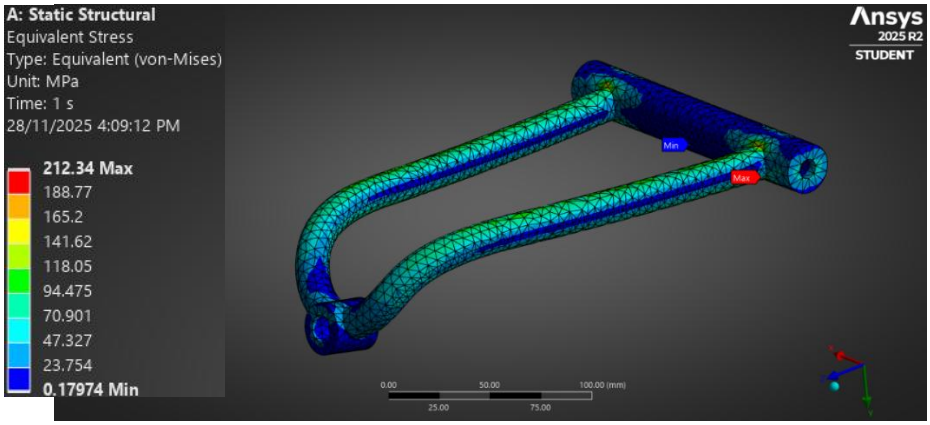

Figure 15: Equivalent stress (von-Mises) distribution under cornering force

Meanwhile, the maximum total deformation occurs at the bottom and front side of the wheel knuckle mounting point and arm, yielding up to a value of 2.499 mm from its

ISSN 2180-1053 e-ISSN 2289-8123 Vol.17 No.2

original position. The minimum total deformation, on the other hand, occurs mostly at the pivot arm and near its welding point, where it experiences zero deformation.

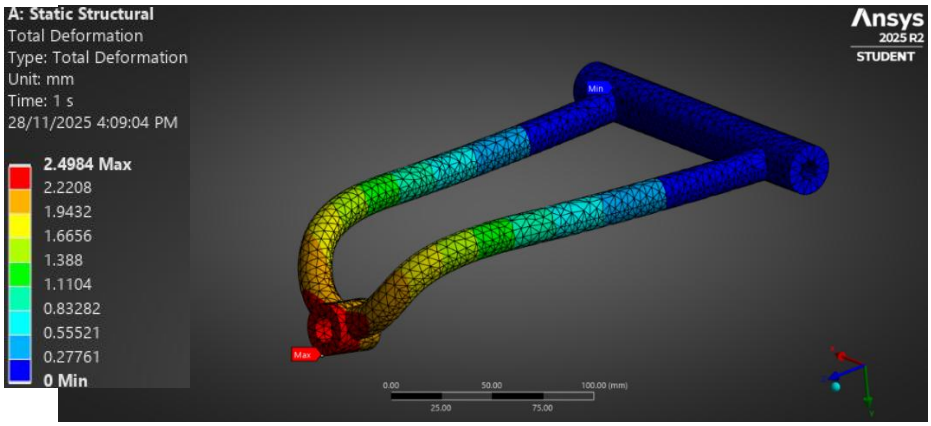

Figure 16: Total deformation distribution under cornering force.

Based on the value of von Mises stress, the minimum Factor of Safety value of 1.17 was also obtained at the underside of the welding point between the upper arm legs and pivot tube. Conversely, the underside of the wheel knuckle connector obtains the highest number of FoS. All in all, the overall FoS values in Figure 17 shows that the upper arm can withstand braking loads under SEM conditions, albeit only by a slight amount.

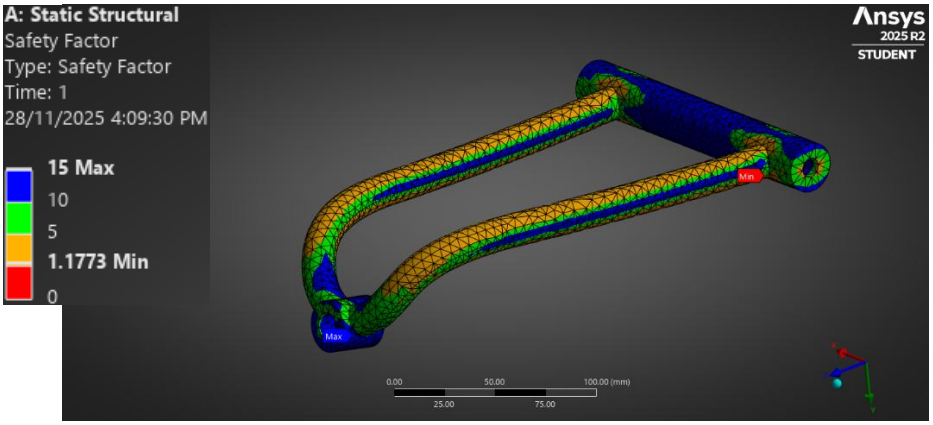

Figure 17: Factor of Safety distribution under cornering force.

4.0 CONCLUSION

In conclusion, the suspension upper arm design and material choice resulted in a structure that can marginally withstand static and dynamic forces under braking and cornering. The results consistently showed that the center of the pivot arm experiences the least amount of stress and deformation, indicating a very strong opportunity for weight reduction using topology optimization. Therefore, the upper arm design needs to be studied further to ensure that it can comply with all SEM rules and regulations yet remains lightweight and strong enough to handle both static and SEM condition loads.

ISSN 2180-1053 e-ISSN 2289-8123 Vol.17 No.2

ACKNOWLEDGEMENTS

The author wishes to sincerely thank Universiti Teknikal Malaysia Melaka (UTeM) notably Mr. Habirafidi Ramly and Mr. Izwan Junoh from Faculty of Mechanical Technology and Engineering (FTKM) UTeM for the warm support throughout the completion of this study.

REFERENCES

[1] Ansys. (2025). *Ansys Student Versions* [Online]. Available: https://www.ansys.com/academic/students. [Accessed: Nov. 28, 2025]

[2] U.S. Department of Energy. (2015). *Lightweight Materials for Cars and Trucks* [Online]. Available: https://www.energy.gov/eere/vehicles/lightweight-aterials-cars-and-trucks [Accessed: Nov. 17, 2025]

[3] E. Ch. Tsirogiannis, G. E. Stavroulakis, and S. S. Makridis, "Electric Car Chassis for Shell Eco Marathon Competition: Design, Modelling and Finite Element Analysis," *World Electric Vehicle Journal,* vol. 10, no. 1, p. 8, Jan. 2019, doi: https://doi.org/10.3390/wevj10010008.

[4] J. R. R. Mackenzie and R. Anderson, "The potential effects of electronic stability control interventions on rural road crashes in Australia: simulation of real-world crashes," Centre for Automotive Safety Research, University of Adelaide, Adelaide, Australia, Nov. 2009.

[5] Shell Eco-marathon. (2025). *Shell Eco-marathon Global Rules & Regulations* [Online]. Available:https://www.shellecomarathon.com/about/global-rules.html [Accessed: Nov. 28, 2025]

[6] W. S. Jie and S. A. Abu Bakar, "Dynamic loading effects on car suspension components during road driving," *Journal of Transport System Engineering*, vol. 10, pp. 27–36, Oct. 2023, doi: https://doi.org/10.11113/jtse.v10.210.

[7] A. R. Shinde, S. S. Wangi, and U. S. Kaur, "Material Optimization of Upper Control Arm for Double Wishbone Suspension System," *International Research Journal of Engineering and Technology (IRJET)*, vol. 07, no. 03, 2020.